

Polydiacetylene Nanofibers Created in Low-Molecular-Weight Gels by Post Modification: Control of Blue and Red Phases by the Odd–Even Effect in Alkyl Chains

Norifumi Fujita,* Yoshimine Sakamoto, Michihiro Shirakawa, Masayoshi Ojima, Akihiko Fujii, Masanori Ozaki, and Seiji Shinkai*

Department of Chemistry and Biochemistry, Graduate School of Engineering, Kyushu University, Fukuoka, 812-8581, Japan, Center for Future Chemistry, Kyushu University, Fukuoka 812-8581, Japan, and Division of Electrical, Electronic and Information Engineering, Graduate School of Engineering, Osaka University Suita, Osaka 565-0871, Japan

Received January 5, 2007; E-mail: nfjtcm@mbox.nc.kyushu-u.ac.jp; seijitcm@mbox.nc.kyushu-u.ac.jp

Diacetylene (DA) is a well-known series of substances that undergoes topochemical reactions upon UV-irradiation or thermal stimuli, leading to the anisotropic formation of polydiacetylene (PDA) in the crystalline state.¹ It is known that strict steric conditions in the arrangement of monomers are required in such topochemical reactions of diacetylene, that is, there must be 4.9 Å of translational distance between the DA units and an inclination angle of 45° between the DA axes.² Recently, numerous studies on the topochemical reactions of DA have been conducted not only in the crystalline states, but also in the mesophases such as in micelles,³ Langmuir–Blodgett films,⁴ and self-assembled monolayers.⁵ Fascination with the features of organogel tissues having one-dimensional elongated morphology with a length of several tens of micrometers and unimolecular width has led to several studies concerning in situ polymerized DA in the organogel system toward construction of electric nanomaterials.^{6,7} In the topochemical polymerization processes of DA in such mesophases, PDA shows either a blue or a red color, depending on the polymerization conditions; however, the origin of the color difference has not yet been well understood. In 1984, Wegner et al. summarized the relationship between the wavelength of the absorbance and the effective conjugation length (ECL) in PDAs.⁸ They found that ECL is strongly affected by the planarity of the main chain of PDA in a linear relationship. According to their analyses, PDAs having an ECL of around 20 mer should show a red color, and those having an ECL of 30 mer should show a blue color. This information implies that the molecular modeling calculation of the stable conformation of PDA is useful in predicting PDA colors.

Recently, we and others have enjoyed low-molecular-weight gel chemistry using cholesterols and substituted gallic acids⁹ as the backbone of gelators.¹⁰ With the above-mentioned goal in mind, we attached the promising gel-forming segments, 3,4,5-trialkoxybenzoic acid moieties, to the DA with flexible alkyl chains (G_n , $n = 3–8$; Figure 1 left). The photopolymerizable unit with flexible linkers is expected to be strongly stabilized by intermolecular hydrogen bondings between two amide linkages that are surrounded by the gel-forming segments. The amide groups are widely used to fix DA in a suitable orientation because the distance between them (about 4.8 Å) is comparable to that of the DA units (about 4.9 Å).

First, we surveyed the stable conformation of 24 mers of G_3 and G_4 by molecular modeling calculation (MMFF94). As seen in Figure 1 right, the radius of the curvature in poly G_3 is shorter than that in poly G_4 , and G_3 may have an ECL shorter than G_4 (also see Figure S1 in Supporting Information). We assumed that the difference in the curvature is attributable to the number of carbon atoms (n) in the alkyl chains in G_n ; that is, the length of the alkyl

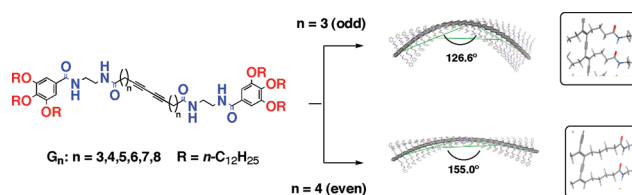


Figure 1. Chemical structure of G_n and the optimized conformation of 24 mers of (upper) poly G_3 and (lower) poly G_4 .

chains and the odd–even effect in the carbon atoms should behave as key factors causing a strain on the alkyl chains in poly G_n s.

To prove these assumptions, we conducted the topochemical reaction of G_n s in the gel state. All the compounds (G_n s) were synthesized using a conventional reaction sequence (Scheme S1). G_n s synthesized here showed fine gelating properties at low concentrations ranging from hydrocarbons to aromatic, alcoholic, and aprotic polar solvents, such as 1,4-dioxane, butyronitrile, and DMF (Table S1). Among them, we selected hexane as a solvent to prepare transparent gels with G_n (for G_3 , Figure S2) for the subsequent topochemical reaction, since transparency is a very important factor in avoiding the reflection of light when the gels are subjected to photochemical reactions. Before the photopolymerization of G_n gels, we performed transmission electron microscopic (TEM) analyses of the hexane gels of G_n s to obtain direct images of the one-dimensional gel tissue. As shown in the TEM image (Figure S3), the elongated one-dimensional assembly reaches to several tens of micrometers long, which is attributed to several 10 000 molecular stacks in the fibrous structure. These observations revealed that the elongated DA assemblies are suitable templates for the anisotropic topochemical reaction of DA in the gel phase.

With such 1-D arrays of polymerizable units in hand, we conducted the photopolymerization of DA in the gel phase. In a typical procedure, the hexane gel (2.5 g dm⁻³) of G_3 in a 5 mm quartz cell was subjected to photoirradiation with a 100 W high-pressure mercury lamp at room temperature from a distance of 5 cm. Upon UV irradiation, the color of the gel immediately changed from transparent to red while retaining its gel state. The time-dependence of the UV–vis spectral change in this photopolymerization process showed that a new absorption band characteristic of PDA appears at 520 nm, which gradually increases and is almost saturated in 3 h (Figure 2a left). Photopolymerization of G_4 in the gel state under the same conditions proceeded smoothly within 3 h, as it did with G_3 , but interestingly, the polymerized sample of G_4 showed a blue color with new absorption bands at 550 and 610 nm (Figure 2a right). From the absorbance, we can estimate these ECL values to be 10 mer for G_3 and 25 mer for G_4 . These results meet our predictions, based on the results obtained by the molecular

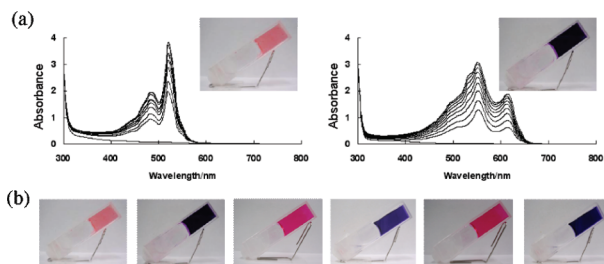


Figure 2. (a) Time-dependence (0–180 min) of UV–vis spectral change on photoirradiation to the hexane gels (2.5 g dm^{-3}) prepared from \mathbf{G}_3 (left) and \mathbf{G}_4 (right), and photographs of the 3-hour-photoirradiated gels (insets); (b) photographs of hexane gels of \mathbf{G}_3 – \mathbf{G}_8 (2.5 g dm^{-3}) after photoirradiation for 3 h.

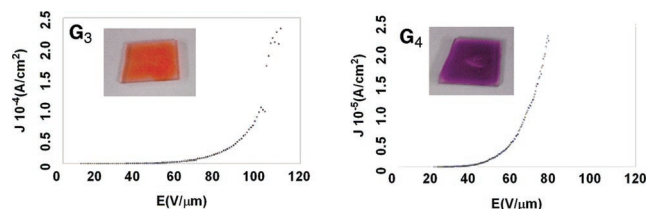


Figure 3. Field emission properties of xerogels prepared from \mathbf{G}_3 and \mathbf{G}_4 on ITO electrodes (inset: photographs of the xerogel-modified ITO electrodes).

modeling of \mathbf{G}_3 and \mathbf{G}_4 , which showed that \mathbf{G}_4 is less affected by steric distortion than \mathbf{G}_3 .¹¹

A similar trend is also seen in the cases of \mathbf{G}_5 – \mathbf{G}_6 and \mathbf{G}_7 – \mathbf{G}_8 . As shown in Figure S5, the spectral patterns can be classified into two categories. The absorption bands of the poly \mathbf{G}_{odds} (\mathbf{G}_{odd} is \mathbf{G}_n with the odd n number) appear at shorter wavelengths (\mathbf{G}_3 , 520 nm; \mathbf{G}_5 , 526 nm; \mathbf{G}_7 , 530 nm), whereas the absorption bands of the poly $\mathbf{G}_{\text{evens}}$ (\mathbf{G}_{even} is \mathbf{G}_n with the even n number) appear at longer wavelengths (\mathbf{G}_4 , 610 nm; \mathbf{G}_6 , 615 nm; \mathbf{G}_8 , 625 nm). These findings reveal that the odd–even effect of the alkyl chains between the DA and the amide moiety significantly governs the planarity of the poly \mathbf{G}_3 –poly \mathbf{G}_8 . Moreover, it is found that the absorption maxima for poly \mathbf{G}_{odds} and poly $\mathbf{G}_{\text{evens}}$ gradually shift to a longer wavelength while increasing n . This observation is fairly understood as follows: the strain in the PDA obtained from \mathbf{G}_n gels is more relaxed from the intermolecular hydrogen bondings between amide groups running along the polydiacetylene main chain with an increase in the number of carbon atoms in the alkyl chains.¹² It is worth emphasizing that the odd–even effect of ECL shown here in poly \mathbf{G}_{odds} and poly $\mathbf{G}_{\text{evens}}$ can be directly detected by the naked eye. As clearly seen in Figure 2b, the color of the \mathbf{G}_{odd} gels is red and that of \mathbf{G}_{even} is blue, as expected. This is a very rare example in which the odd–even effect of the linkages appears very clearly.

ECL in conductive polymers should strongly affect their photonic and electric properties. On the basis of several preliminary experiments, we noticed that the gel fibers with a very thin morphology can become potential candidates for electric field emission material. The PDA prepared here has a fibrous morphology with a high aspect ratio and is expected to have a certain degree of conductivity. To begin, we conducted an evaluation of the field emission properties of the thin film prepared from poly \mathbf{G}_3 and poly \mathbf{G}_4 . The ethanol gels (10 g dm^{-3}) were cast on ITO electrodes, and the gel-modified ITO electrodes were photoirradiated for 3 h to complete the photopolymerization of DA (Figure 3 inset). The progress of the photopolymerization could be easily monitored from the color change. The field emission measurements were performed with the gel-modified ITO electrodes as emitters in a high-vacuum chamber (10^{-7} Torr).¹³ Figure 3 shows the field emission current

density of the gel fiber-coated ITO electrodes prepared from \mathbf{G}_3 and \mathbf{G}_4 . It is noteworthy that the electrode prepared from \mathbf{G}_4 has a turn-on field ($35 \text{ V}/\mu\text{m}$) lower than that of \mathbf{G}_3 ($50 \text{ V}/\mu\text{m}$). One can reasonably attribute this to the difference of ECL between \mathbf{G}_3 and \mathbf{G}_4 .

In conclusion, we have demonstrated that molecular modeling to seek a stable conformation of PDA prepared from \mathbf{G}_n s in the gel state is useful in predicting the ECL in PDA where the odd–even number of alkyl chains (n) is a key factor for determining the blue and red phases of the PDAs. These findings should prove useful in the design of PDA-based sensors for organic and biomolecular objectives as well as conductive materials for nano-wires and nanodevices.

Acknowledgment. Support was provided by Grants-in-Aid (No. 16750122, 15105004, and 18033040), the 21st Century COE Project, and The Mitsubishi Foundation.

Supporting Information Available: Syntheses and gelation properties of \mathbf{G}_n , UV–vis and IR spectra and TEM and AFM images of poly \mathbf{G}_n . This material is available free of charge via the Internet at <http://pubs.acs.org>.

References

- (1) Wegner, G. Z. *Naturforsch., B: Chem. Sci.* **1969**, *24*, 824.
- (2) (a) Baughman, R. H.; Yee, K. C. *J. Polym. Sci. Macromol. Rev.* **1978**, *13*, 219. (b) Enkelmann, V. *Adv. Polym. Sci.* **1984**, *63*, 91.
- (3) (a) Kim, J.-M.; Ji, E.-K.; Woo, S. M.; Lee, H.; Ahn, D. J. *Adv. Mater.* **2003**, *15*, 1118–1121. (b) Lu, Y.; Yang, Y.; Sellinger, A.; Lu, M.; Huang, J.; Fan, H.; Haddad, R.; Lopez, G.; Burns, A. R.; Sasaki, D. Y.; Shelnutt, J.; Brinker, C. J. *Nature* **2001**, *410*, 913–917. (c) Okada, S.; Peng, S.; Spevak, W.; Charych, D. *Acc. Chem. Res.* **1998**, *31*, 229–239. (d) Spevak, W.; Nagy, J. O.; Charych, D. H.; Schaefer, M. E.; Gilbert, J. H.; Bednarski, M. D. *J. Am. Chem. Soc.* **1993**, *115*, 1146–1147. (e) Singh, A.; Thompson, R. B.; Schnur, J. M. *J. Am. Chem. Soc.* **1986**, *108*, 2785–2787.
- (4) (a) Berman, A.; Ahn, D. J.; Lio, A.; Salmerson, M.; Reichert, A.; Charych, D. *Science* **1995**, *269*, 515–518. (b) Tieke, B.; Graf, H. J.; Wegner, G.; Naegele, B.; Ringsdorf, H.; Banerjee, A.; Day, D.; Lando, J. B. *Colloid Polym. Sci.* **1977**, *255*, 521–531. (c) Kuriyama, K.; Kikuchi, H.; Kajiyama, T. *Langmuir* **1998**, *14*, 1130–1138.
- (5) Batchelder, D. N.; Evans, S. D.; Freeman, T. L.; Haessling, L.; Ringsdorf, H.; Wolf, H. *J. Am. Chem. Soc.* **1994**, *116*, 1050–1053.
- (6) Recent reviews: (a) Terech, P.; Weiss, R. G. *Chem. Rev.* **1997**, *97*, 3133–3159. (b) van Esch, J.; Schoonbeek, F.; de Loos, M.; Kooijman, H.; Veen, E. M.; Kellogg R. M.; Feringa, B. L. In *Supramolecular Science: Where It Is and Where It Is Going*; Ungaro, R., Dalcanale, E., Eds.; Kluwer: The Netherlands, 1999; p 233. (c) Shinkai, S.; Murata, K. *J. Mater. Chem.* **1998**, *8*, 485. (d) Gronwald, O.; Shinkai, S. *Chem.–Eur. J.* **2001**, *7*, 4329. (e) Fages, F., Ed. *Low Molecular Mass Gelators*. In *Topics in Current Chemistry*; Springer-Verlag: Berlin, Germany, 2005; Vol. 256. (f) Weiss, R. G.; Terech, P., Eds. *Molecular Gels*; Springer: The Netherlands, 2006. (g) George, M.; Weiss, R. G. *Acc. Chem. Res.* **2006**, *39*, 489.
- (7) (a) Inoue, K.; Ono, Y.; Kanekiyo, Y.; Hanabusa, K.; Shinkai, S. *Chem. Lett.* **1999**, 429–430. (b) Masuda, M.; Hanada, T.; Yase, K.; Shimizu, T. *Macromolecules* **1998**, *31*, 9403–9405. (c) Tamaoki, N.; Shimada, S.; Okada, Y.; Belaisaoui, A.; Kruk, G.; Yase, K.; Matsuda, H. *Langmuir* **2000**, *16*, 7545–7547. (d) George, M.; Weiss, R. G. *Chem. Mater.* **2003**, *15*, 2879–2888. (e) Shirakawa, M.; Fujita, N.; Shinkai, S. *J. Am. Chem. Soc.* **2005**, *127*, 4164–4165.
- (8) Wenz, G.; Müller, M. A.; Schmit, M.; Wegner, G. *Macromolecules* **1984**, *17*, 837–850.
- (9) (a) See ref 6a. (b) Sugiyasu, K.; Fujita, N.; Shinkai, S. *Angew. Chem., Int. Ed.* **2004**, *43*, 1229–1233. (c) Kawano, S.-i.; Fujita, N.; Shinkai, S. *J. Am. Chem. Soc.* **2004**, *126*, 8592–8593. (d) Kawano, S.-i.; Fujita, N.; Shinkai, S. *Chem.–Eur. J.* **2005**, *11*, 4735–4742.
- (10) (a) Mukhopadhyay, P.; Iwashita, Y.; Shirakawa, M.; Kawano, S.-i.; Fujita, N.; Shinkai, S. *Angew. Chem., Int. Ed.* **2006**, *45*, 1592. (b) Kitahara, K.; Shirakawa, M.; Kawano, S.-i.; Beginn, U.; Fujita, N.; Shinkai, S. *J. Am. Chem. Soc.* **2005**, *127*, 14980. (c) Shirakawa, M.; Fujita, N.; Tani, T.; Kaneko, K.; Shinkai, S. *Chem. Commun.* **2005**, 4149.
- (11) AFM observation of the poly \mathbf{G}_3 and poly \mathbf{G}_4 prepared in the gel state revealed that unimolecular fibers have more than a few microns in length which is fairly longer than those estimated by ECL (Figure S6).
- (12) IR spectral analyses on the hexane gels of \mathbf{G}_3 and \mathbf{G}_4 (2.5 g dm^{-3}) revealed that absorption bands appear at 1633 and 1544 cm^{-1} , which are characteristic of hydrogen bonded amide I and amide II, respectively, before and after photoirradiation (Figure S7).
- (13) Ojima, M.; Hiwatashi, S.; Araki, H.; Fujii, A.; Ozaki, M.; Yoshino, K. *Appl. Phys. Lett.* **2006**, *88*, 053103.

JA069307+